DMD Fast Forward. Published on October 18, 2006 as doi:10.1124/dmd.106.011734

DMD #11734

Humanized IgG_1 Variants With Differential Binding Properties To The Neonatal Fc Receptor: Relationship To Pharmacokinetics In Mice And Primates

Amita Datta-Mannan, Derrick R. Witcher, Ying Tang, Jeffry Watkins, Weidong Jiang and Victor J. Wroblewski

Departments of Drug Disposition Development/Commercialization (A.D-M., V.J.W.) and Biotechnology Discovery Research (D.R.W.), Lilly Research Laboratories, Lilly Corporate Center, Indianapolis, Indiana. Discovery Research (Y.T., J.W.) Applied Molecular Evolution, San Diego, California. Discovery Research (W.J.) VasGene Therapeutics, Los Angeles, California

Running Title: Neonatal Fc Receptor Binding and Pharmacokinetics of IgG_1s

Address Correspondence to: Victor J. Wroblewski, Lilly Research Laboratories, Eli Lilly & Company, Lilly Corporate Center, Indianapolis, IN 46285, Phone: (317) 276-9306, Fax: (317) 276-4218, Email: wroblewski_victor@lilly.com

Number of text pages: 28

Number of tables: 5

Number of figures: 5

Number of references: 33

Number of words in the Abstract: 206

Number of words in the Introduction: 750

Number of words in the Discussion: 1500

List abbreviations: FcRn, neonatal Fc receptor; β_2m, β_2-microglobulin; MCH, major histocompatibility complex; IgGs, immunoglobulins; $t_{1/2\beta}$, terminal phase half-life; TNFα, anti-tumor necrosis factor alpha; WT, wild-type; H-FcRn, human FcRn; C-FcRn, cynomolgus monkey FcRn; M-FcRn, murine FcRn; CHO, Chinese hamster ovarian; PBS, phosphate-buffered saline; IMAC, immobilized metal-affinity column; SPR, surface plasmon resonance; pH_{50}, pH at which 50% of the FcRn-antibody complexes dissociate; ELISA, enzyme linked immunosorbent assay; HRP, horseradish peroxidase; IV, intravenous; K_D, equilibrium dissociation constant; $t_{1/2}$, dissociation half-life; $AUC_{0-\infty}$, area under the plasma concentration curve from zero to infinity; C_{max}, maximal observed plasma concentration; CL, clearance; V_{ss}, volume of distribution at steady state; k_{on}, association rate; k_{off}, dissociation rate

Abstract

It is well established that the neonatal Fc receptor (FcRn) plays a critical role in regulating immunoglobulin (IgG) homeostasis *in vivo*. As such, modification of the interaction of IgG with FcRn has been the focus of protein engineering strategies designed to generate therapeutic antibodies with improved pharmacokinetic properties. In the current work, we characterized differences in interaction of IgG between mouse and primate receptors using three humanized anti-TNFα antibodies with variant IgG_1 Fc regions. The wild-type and variant IgGs demonstrated a differential combination of improved affinity, modified dissociation kinetics and altered pH-dependent complex dissociation when evaluated on the primate and murine receptors. The observed *in vitro* binding differences within and between species allowed us to more completely relate these parameters to their influence on the *in vivo* pharmacokinetics in mice and cynomolgus monkeys. The variant antibodies have different pharmacokinetic behavior in cynomolgus monkeys and mice which appears to be related to the unique binding characteristics observed with the murine receptor. However, we did not observe a direct relationship between increased binding affinity to the receptor and improved pharmacokinetic properties for these molecules in either species. This work provides further insights into how the FcRn:IgG interaction may be modulated to develop monoclonal antibodies with improved therapeutic properties.

FcRn is a heterodimeric protein consisting of a soluble light chain (β_2-microglobulin or β_2m) and a transmembrane anchored heavy chain (α-FcRn). FcRn functions as a "salvage receptor" regulating levels of circulating IgGs in rodents (Ghetie et al., 1996; Junghans and Anderson, 1996). FcRn is expressed ubiquitously in endothelial cells of human tissues (Ghetie and Ward, 2000), and it has been speculated that FcRn also plays a key role in IgG homeostasis in humans (Ghetie et al., 1996; Kim et al., 1999).

Earlier studies demonstrate that the FcRn:IgG interaction is highly pH-dependent. IgG binds to FcRn via the Fc region at pH 6.0 (Raghavan and Bjorkman, 1996; Rodewald, 1976), does not bind to FcRn at neutral pH and the dissociation of the FcRn:IgG complex is facilitated at pH 7.4 (Raghavan et al., 1995; Raghavan and Bjorkman, 1996; Rodewald, 1976). In endothelium, FcRn appears to have an exclusively intracellular localization, within acidified endosomes (Ober et al., 2004a). These observations and cellular studies have suggested of a model of IgG homeostasis, which involves the uptake of IgG into the cell via fluid phase pinocytosis with subsequent binding to FcRn in endosomes (Ober et al., 2004b; Ward et al., 2003). Unbound IgG is directed down a degradative pathway resulting in proteolysis in lysosomes, whereas, FcRn bound antibody is recycled to the cell surface where the neutral pH facilitates dissociation and release into the circulation (Ward et al., 2003).

As monoclonal antibodies continue to show promise as therapeutic agents, there have been a number of studies which have attempted to characterize the *in vivo* influence of Fc mutations which affect the affinity or pH dependence of this receptor interaction (Dall'Acqua et al., 2002; Ghetie et al., 1997; Kim et al., 1994). Optimizing this interaction may lead to the development of superior therapeutic antibodies through

modulation of their pharmacokinetic and/or phamacodynamic properties. Studies have suggested that mutations which increase the affinity of the IgG:FcRn interaction at pH 6.0 result in an improvement in the terminal phase half-life ($t_{1/2\beta}$) of an antibody *in vivo* (Ghetie et al., 1997; Hinton et al., 2004; Hinton et al., 2006; Kim et al., 1994; Medesan et al., 1998), although recent studies have questioned this observation (Dall'Acqua et al., 2002; Gurbaxani et al., 2005). Other investigations suggest that modulation of the affinity of IgG for FcRn interaction at neutral pH is an important consideration (Dall'Acqua et al., 2002; Hinton et al., 2004). It is likely that optimization of the pharmacokinetics thru FcRn will need to consider a combination of these properties.

In the current work, we have developed a series of humanized anti-tumor necrosis factor alpha (TNFα) IgG_1 Fc variants which show a combination of *in vitro* FcRn binding properties. The variants were built on a TNFα backbone, with the intent of eliminating/limiting the influence of antigen binding on the kinetics or distribution of the antibody. The mutations made in the wild-type (WT) Fc sequence were: P257I/Q311I, P257I/N434H and D376V/N434H[1]. These variants demonstrated differential *in vitro* binding properties against human (H-FcRn), cynomolgus monkey (C-FcRn) and murine FcRn (M-FcRn), which allowed us to correlate *in vitro* binding properties to the *in vivo* pharmacokinetic behavior of these molecules in mice and cynomolgus monkeys. Each of the variants bound with greater affinity (~15- to 197-fold) to H-FcRn, C-FcRn and M-FcRn at pH 6.0, but showed no direct binding at neutral pH (7.4). After formation of the antibody:M-FcRn complexes at pH 6.0, we observed a decrease in the proportion of the variant IgGs dissociating from M-FcRn with increasing pH, which was not evident after formation of the C-FcRn: or H-FcRn:IgG complexes. In cynomolgus monkeys, the

molecules demonstrated similar pharmacokinetic behavior suggesting that increased binding affinity at pH 6.0 is not enough to result in improved pharmacokinetic properties for these molecules. After administration to mice, we observed an increased clearance of each of the variant IgGs from the circulation relative to the WT antibody. The pharmacokinetics in mice suggest the proportion of each variant IgG released from M-FcRn at the neutral pH of the cell surface is less than the WT molecule, consistent with the differential pH dependent release we observed *in vitro*. These findings suggest that even subtle influences on the pH dependence of the FcRn:IgG dissociation of these variant molecules may influence how an antibody is processed by the recycling pathway. Our results demonstrate that a systematic assessment of the multiple parameters of FcRn:IgG interaction both within and between species allows one to assess the relationship of FcRn-mediated antibody trafficking to *in vivo* IgG performance.

Methods

Cell culture

293EBNA cells were maintained at 37 °C under 5-8% CO_2 conditions in Dulbecco's modified Eagle's medium/F-12 (Gibco) supplemented with 20mM HEPES, 5 μg/mL nucellin, 0.4 μg/mL tropolone, 0.075% (w/v) F68 and 50 μg/mL Geneticin.

Chinese hamster ovarian (CHO)-K1 cells were maintained at 37 °C under 5-8% CO_2 conditions in Dulbecco's modified Eagle's medium/F-12 (Gibco) supplemented with 10% FBS.

Cloning, expression and purification of H-FcRn, C-FcRn and M-FcRn

The genes encoding for the soluble portion of the heavy subunit of M-FcRn (residues 1 to 276), H-FcRn (residues 1 to 268), murine β_2m and human β_2m were constructed by Geneart GmbH (Regensburg, Germany) and subsequently subcloned into cytomegalovirus expression vectors. The heavy subunits and β_2m containing plasmids were cotransfected at a 3:1 ratio, respectively, into 293EBNA cells using XtremeGene (Roche). H-FcRn and M-FcRn were purified from supernatants using pH-dependent binding to separate columns packed with IgG Sepharose™ 6 Fast Flow (GE Healthcare). Prior to loading, the pH of the supernatants was adjusted to 6.0 and the columns were equilibrated with 50 mM $NaPO_4$, pH 6.0, to capture the receptors. After loading, the IgG columns were washed with 50 mM $NaPO_4$, pH 6.0 until the absorbance returned to baseline and the bound receptors were eluted with 50 mM $NaPO_4$, pH 7.4. Fractions containing the receptors were pooled and further purified by size exclusion chromatography on a Superdex 200 column (GE Healthcare) with 50 mM $NaPO_4$, pH 7.4 as the running buffer. Fractions containing H-FcRn or M-FcRn were pooled, and

characterized by SDS-PAGE and mass spectrometry. Samples were dialyzed into PBS (1 mM potassium phosphate, 3 mM sodium phosphate, 0.150 M NaCl), pH 7.4, dispensed into single use aliquots and stored at -20°C.

The genes encoding for the heavy subunit of C-FcRn (residues 1-299) and cynomolgus monkey β_2m were cloned by PCR using cDNA from cynomolgus monkey peripheral blood mononuclear cells. A His_6-tag was added to the 3'-end of heavy chain and each gene was subcloned into cytomegalovirus expression vectors. The heavy subunit and cynomolgus monkey β_2m were co-transfected at a 1:1 ratio into CHO-K1 cells using Lipofectamine 2000 (Invitrogen) and cells expressing the receptor were selected in serum-free Ultraculture medium (Cambrex Bio Science Walkersville, Inc) containing 25 μM methotrexate. C-FcRn was purified from cell supernatants by immobilized metal-affinity chromatography (IMAC) using a HisTrap™ column (GE Healthcare). Prior to loading, the pH of the supernatant was adjusted to 7.0 and the columns were equilibrated with 20 mM $NaPO_4$, 500 mM NaCl, 200 mM arginine, pH 7.0 (Buffer A), to capture the receptor. After loading, the IMAC column was washed with Buffer A until the absorbance returned to baseline and the bound C-FcRn was eluted using a linear gradient of 0 M to 0.5 M imidazole (dissolved in Buffer A). Fractions containing C-FcRn were pooled and further purified by anion exchange chromatography using a HiPrep™ Sepharose column (GE Healthcare) with 50 mM $NaPO_4$, pH 7.4 as the running buffer. Fractions containing C-FcRn were pooled and characterized by SDS-PAGE. Samples were dialyzed into PBS, pH 7.4, dispensed into single use aliquots and stored at -80°C.

Construction of the IgG Fc library

Humanized IgG_1 Fc variant libraries were created using a Kunkel-based strategy (Kunkel et al., 1987)) with oligonucleotides designed to mutate a single Fc residue in the clone to each of the eighteen non-wild-type amino acids (cysteine was excluded). Briefly, in a 96-well PCR plate, the oligonucleotide for each variant was individually annealed to a uridinylated IgG_1 heavy chain (γ_1) template at a 50:1 ratio by denaturing at 85°C for 1 min, cooling to 45°C over 30 min, then chilling to 4°C. After addition of T7 DNA polymerase, T4 DNA ligase and synthesis buffer (31), the synthesis reaction was carried out at 37°C for 2 hours. A small aliquot of the reaction was then transformed into *E. coli* XL-1 cells (Stratagene). Individual colonies were picked for plasmid preparation and DNA sequencing to identify clones with designed Fc mutations.

The IgGs were expressed from transiently transfected CHO-K1 cells. The concentration of IgG in the culture supernatant was determined by an enzyme-linked immunosorbent assay (ELISA) using light and heavy chain detection antibodies.

Following IgG quantification, the concentration of Fc variant in the supernatant was normalized with mock medium, the pH was adjusted to 6.0 with FcRn-binding buffer (100 mM $NaPO_4$, 0.05% Tween-20, pH 6.0) and assayed in duplicate for binding to recombinant H-FcRn at pH 6.0. Single mutation variants which displayed an enhanced H-FcRn binding at pH 6.0 relative to the wild-type IgG were identified and further characterized for concentration dependent H-FcRn binding at pH 6.0 and pH 7.4.

Data from the interaction of H-FcRn with the single mutants was used to guide the synthesis of IgG variants with two amino acid mutations in the Fc region by Kunkel mutagenesis (Kunkel et al., 1987). The double mutants were expressed as described above and assayed for H-FcRn binding at pH 6.0 and pH 7.4. Three variants which

DMD Fast Forward. Published on October 18, 2006 as DOI: 10.1124/dmd.106.011734
This article has not been copyedited and formatted. The final version may differ from this version.

displayed enhanced H-FcRn binding at pH 6.0 (relative to the WT molecule) and minimal impact on the direct binding interaction at pH 7.4 were converted to a humanized anti-TNFα IgG_1 by Fab-Fc gene ligation and fully characterized as described below. The anti-TNFα IgG_1 platform allowed the study of pharmacokinetics in normal primates or mice with minimal or no influence of antigen driven clearance.

Expression and Purification of IgGs

The WT anti-TNFα antibody and Fc variants, P257I/N434H, P257I/Q311I and D376V/N434H, were expressed in 293EBNA cells and purified using one of the two following methods.

Expression media from 293EBNA cells was concentrated and loaded directly onto an IMAC column (GE Healthcare) at a flow rate of 5 mL/min. The column was washed with buffer A (1 mM potassium phosphate, 3 mM sodium phosphate, 0.150 M NaCl, pH 7.4) until the absorbance returned to baseline and the bound antibodies were eluted with a linear gradient from 0 M to 0.225 M imidazole (dissolved in buffer A) over 60 minutes. Fractions containing the anti-TNFα antibody variants were pooled and dialyzed against 25 mM phosphate, 50 mM NaCl, pH 7.4 (Buffer B). The dialysates were then concentrated and loaded onto a Superdex 200 (Pharmacia, 26/60) sizing column equilibrated with Buffer B, at a flow rate of 3 mL/min. Fractions containing antibody were pooled and characterized by SDS-PAGE and mass spectrometry. Samples were sterile filtered (0.22 μm) and stored at 4 ^{o}C.

For the second purification method, expression media from 293EBNA cells containing the expressed anti-TNFα antibodies were concentrated and loaded onto a recombinant Protein-A Sepharose pre-packed column (GE Healthcare) at a rate of 5

mL/min. The column was washed with Buffer A until the absorbance returned to baseline. The antibodies were eluted with 100 mM glycine, pH 3.2, and fractions were neutralized using 40 µl Tris (pH 8.0) per milliliter of elution buffer. Fractions containing the antibodies were pooled and concentrated and loaded onto a Superdex 200 (GE Healthcare 26/60) sizing column equilibrated with Buffer A at a flow rate of 3 mL/min. Fractions containing antibody were pooled and characterized by SDS-PAGE and mass spectrometry. Samples were sterile filtered (0.22 µm) and stored at 4 ^{o}C.

Labeled FcRn preparation

Fluorescently labeled M-FcRn and C-FcRn for anisotropy measurements were obtained by reaction of the purified soluble proteins with Alexa 488 (Molecular Probes) using the vendor recommended reaction conditions. The number of moles of Alexa 488 per mole of each FcRn was determined spectrophotometrically as 2.0 and 1.3 moles for C-FcRn and M-FcRn, respectively. Biotinylated H-FcRn, M-FcRn and C-FcRn for ELISA assays were produced by reacting each purified soluble protein with EZ-Link® Sulfo-NHS-Biotin (Pierce Chemical Co.) using the conditions supplied by the vendor. The FcRn:biotin ratio for H-FcRn, M-FcRn and C- FcRn were measured as 1.1, 1.2 and 1.1, respectively, using the EZ™ Biotin Quantitation Kit (Pierce Chemical Co.).

Surface plasmon resonance (BIAcore) measurements

Surface plasmon resonance (SPR) measurements were performed on a BIAcore 2000 instrument using a CM5 sensor chip (Biacore Inc.). H-FcRn, C-FcRn and M-FcRn were immobilized to flow cells 2, 3 and 4, respectively, of the sensor chip using amine-coupling chemistry. The flow cells were activated for 7 min with a 1:1 mixture of 0.1 M N-hydroxysuccinimide and 0.1 M 3-(*N*,*N*-dimethylamino)propyl-*N*-ethylcarbodiimide at

a flow rate of 5 µL/min. H-FcRn (4 µg/mL in 10 mM sodium acetate, pH 5.5), C-FcRn (5 µg/mL in 10 mM sodium acetate, pH 5.5) and M-FcRn (3 µg/mL in 10 mM sodium acetate, pH 5.5) were injected over flow cells 2, 3 and 4, respectively, for 15 min at 5 µL/min, which resulted in a surface density of 200-300 response units (RU) for each receptor. Surfaces were blocked with a 7 min injection of 1 M ethanolamine-HCl, pH 8.5. Flow cell 1 was used as a control surface without FcRn and was prepared similarly to sample flow cells. The data from this "blank" flow cell were subtracted from the sample data.

Kinetic SPR experiments for each antibody were carried out at a flow rate of 100 µL/min and a sampling rate of 1 Hz. Sensorgrams were collected for all antibodies dissolved in PBS, pH 6.0 and 0.005% (v/v) Tween 20 at 25°C over a concentration range of 0.0033 to 4 µM. The running buffer used in the experiments was the same as the antibody diluent buffer. Signals were monitored as flow cell 2 minus flow cell 1 for H-FcRn:antibody interactions, flow cell 3 minus flow cell 1 for C-FcRn:antibody interactions and flow cell 4 minus flow cell 1 for M-FcRn:antibody interactions. One 30 second pulse of PBS, pH 7.4 was used to regenerate the surfaces. Kinetic binding constants for the antibody:FcRn interactions were determined from data recorded at various antibody concentrations by using the program BIAevaluation, version 3.1. Global fits were determined from an average of two data sets collected on separate days. k_{on} (association rate) and k_{off} (dissociation rate) were simultaneously fit to a heterogeneous binding model (Martin and Bjorkman, 1999) to determine K_D (equilibrium dissociation constant) values. Curve fits for both association and dissociation phases of the sensorgrams showed low χ^2 values and low residuals.

DMD Fast Forward. Published on October 18, 2006 as DOI: 10.1124/dmd.106.011734
This article has not been copyedited and formatted. The final version may differ from this version.

Fluorescence anisotropy pH-dependent dissociation assay for the WT, P257I/N434H, P257I/Q311I and D376V/N434H anti-TNFα antibodies

Anisotropy measurements of Alexa 488 (Molecular Probes) labeled M-FcRn and C-FcRn were recorded at 25°C on a ISS PC-1 fluorometer by using excitation and emission wavelengths of 494 and 519 nm, respectively. Alexa 488-FcRn was premixed with antibody to 75% saturation in PBS, pH 6.0. For the displacement of Alexa 488-FcRn from antibody, increasing amounts 0.25 M NaOH were added, while monitoring the pH with an electrode. Displacement curves were analyzed by a four-parameter nonlinear regression fit (Sigma Plot v8, SPSS Inc.) to determine the midpoint (pH_{50}) of the titration curve (the pH at which 50% of the Alexa 488-FcRn:antibody complexes dissociates).

pH-dependent dissociation enzyme-linked immunosorbent assay (ELISA) for the WT, P257I/N434H, P257I/Q311I and D376V/N434H anti-TNFα antibodies

Greiner Microlon ELISA plates were coated with 0.005 μg/well of Neutravidin (Pierce Chemical Co.) diluted in 50 mM carbonate buffer, pH 9.3, at 4°C overnight. After washing and blocking, 0.5 μg of biotinylated H-FcRn, C-FcRn or M-FcRn were added to each well and allowed to bind the neutravidin-coated wells for 1 h at 25°C. Wells were washed after FcRn binding and 0.05 μg/well of anti-TNFα antibody, dissolved in 100 mM $NaPO_4$, pH 6.0, 0.05% Tween 20 (v/v), 0.1% ovalbumin (m/v), was added to each well and incubated for 1 h at 25°C. Following antibody binding, wells were washed three times with 10 or 30 minute incubations at 25°C between each wash using 100 mM $NaPO_4$, 0.05% Tween 20 (v/v) buffer having pH values from 6.0 to 8.0 in 0.2 pH increments. The remaining bound anti-TNFα antibodies were detected with a horseradish peroxidase (HRP)-conjugated goat $(Fab')_2$ anti-human-Fab (Jackson Labs).

Optical density data were analyzed by the same four-parameter nonlinear regression fit as the fluorescence anisotropy data. The amount of antibody which remained bound at each pH was expressed as a percentage of the total antibody bound at pH 6.0.

Cynomolgus monkey pharmacokinetic study

Nine male cynomolgus monkeys (2.8-3.8 kg) were assigned to one of three study groups. Each animal received a single intravenous (IV) dose of anti-TNFα WT, P257I/N434H or D376V/N434H dissolved in PBS, pH 7.4, at 0.5 mg/kg. Blood samples were collected from the femoral vein prior to dosing and at 0.25, 0.5, 1, 3, 6, 12, 24, 48, 72, 96, 120, 168, 240, 312, 384, 456 and 528 hours after administration of the dose. Blood samples were allowed to clot at ambient temperature prior to centrifugation to obtain serum.

Murine pharmacokinetic studies

Pharmacokinetic analyses for anti-TNFα WT, P257I/Q311I, P257I/N434H and D376V/N434H were conducted in male CD-1 (20-30 g) (Harlan, Indianapolis, IN) and male B6 (C57BL/6J; 15-20 g) (Jackson Laboratories, Bar Harbor, ME) mice. A single IV dose of the anti-TNFα WT, P257I/Q3111I, P257I/N434H or D376V/N434H dissolved in PBS, pH 7.4 was administered, via the tail vein, at a dose level of 1 mg/kg. Blood samples were collected from three or four animals per treatment group per time point at 0.08, 0.25, 1, 6, 12, 24, 72, 96, 144, 168, 192, 216, 288, 360 and 432 h after administration. The samples were collected by saphenous vein or by tail clip into tubes containing potassium EDTA as anticoagulant and processed to plasma.

Bioanalytical Assays

Concentrations of the WT anti-TNFα and the P257I/Q311I, P257I/N434H and D376V/N434H variants in cynomolgus monkey and murine samples were determined using a validated anti-human IgG_1 and/or antigen capture (with TNFα, R&D Systems) ELISAs. Briefly, for the antigen capture ELISA, each well of a Immulon 4 microtiter plate (Thermo Electron Corporation) was coated with 0.1 µg TNFα at 4°C overnight; for the anti-human IgG_1 ELISA, each well was coated with 0.2 µg of a goat anti-human kappa light chain antibody. After washing and blocking, standards and samples were added to the wells in a volume of 0.1 mL and incubated for 1 h at room temperature. Standards (anti-TNFα WT, P257I/Q311I, P257I/N434H and D376V/N434H) were prepared in either cynomolgus monkey serum or mouse plasma (EDTA) and study samples were diluted in the appropriate matrix. After washing, the bound antibodies were detected with a HRP-conjugated mouse anti-human light chain antibody (Southern Biotechnology Associates, Birmingham, AL). The standard curve range in both assay formats for anti-TNFα WT and D376V/N434H was from 0.78 to 50 ng/mL and the lower limit of quantitation was defined as 2 ng/mL. For P257I/Q3111I and P257I/N434H the standard curve range in both assay formats was from 1.56 to 100 ng/mL and the lower limit of quantitation was defined as 4 ng/mL.

Pharmacokinetic data analysis

Pharmacokinetic parameters were calculated using WinNonlin Professional (Version 3.2) software package (Pharsight Corporation, Mountain View, CA). Serum concentration-time data were calculated using a model-independent approach based on the statistical moment theory. The parameters calculated included the area under the

curve ($AUC_{0-\infty}$), clearance (CL), volume of distribution (V_{ss}) and elimination half-life ($t_{1/2\beta}$).

Statistical analyses

Statistical differences in PK parameters for the wild-type and Fc variants in cynomolgus monkey were determined using standard analysis of variance (ANOVA) methods. *In vitro* binding data (K_D and pH_{50}) were also analyzed using ANOVA. For mouse plasma concentration data a linear mixed effect model was used which included time-by-group and quadratic terms for time-by-group as fixed effects.

Results

Binding affinities and interaction kinetics of the anti-TNFα antibodies with FcRn

The IgG library carrying single or double Fc mutations was initially screened for binding to H-FcRn at pH 6.0 and pH 7.4 using an FcRn ELISA. It is possible that mutation of residues in the Fc critical to maintaining the pH dependency of receptor binding at pH 6.0 and release at pH 7.4 could generate variants with enhanced affinity at both pH values. The IgG:FcRn interaction was measured at both pH values to ensure that the variants displayed the characteristic receptor affinity at pH 6.0 and minimal interaction at pH 7.4. The variants which displayed the greatest binding enhancement to H-FcRn at pH 6.0 relative to WT with insignificant interaction at pH 7.4 were selected for further interaction characterization with C-FcRn and M-FcRn. The variants which displayed improved FcRn affinity at pH 6.0 compared to WT with no significant binding at pH 7.4, across the three species of receptors, included P257I/Q311I, P257I/N434H and D367V/N434H. While the binding ELISA was used as a screen for ranking the relative affinity improvements, a more complete understanding of the interaction with FcRn requires consideration of the equilibrium dissociation constants (K_D values) and binding kinetics (k_{on} and k_{off} values) of each of the antibodies. We measured these parameters for our WT and three humanized Fc variant anti-TNFα IgG_1 antibodies by SPR using high flow rates (100 μL/min) and a low density of surface immobilized FcRn (~250 RU) to avoid mass transport effects on the receptor:IgG interaction. Sensorgrams for the interactions of the WT anti-TNFα and P257I/N434H variant with H-FcRn, C-FcRn and M-FcRn at pH 6.0, are representative of the other variants (Figure 1). Since the association and dissociation phases of the IgG interactions with human FcRn were too

fast for an accurate calculation of K_D values through global fitting, equilibrium binding data were used. A non-interacting two-site binding model which has been reported previously to describe the rat FcRn:Fc interaction (Martin and Bjorkman, 1999) was used to determine the rate constants and K_D values for the interaction of the IgGs with C-FcRn and M-FcRn.

The binding affinity (K_D) of the WT antibody for H-FcRn, C-FcRn and M-FcRn was 37 ± 5 nM, 209 ± 11 nM and 118 ± 7 nM, respectively (Tables 1-3). Compared to the WT antibody, the mutants display enhanced binding to H-FcRn, C-FcRn and M-FcRn at pH 6.0 in the SPR assays (Tables 1-3). Importantly, none of the variants tested bound at detectable levels to the FcRn of any species tested at pH 7.4 when a concentration of 4 μM IgG (the highest concentration measured for pH 6.0 binding) was flowed over the FcRn chip (data not shown). The variants thereby maintained the characteristic pH dependence of the receptor:IgG interaction critical for regulating the persistence and levels of IgG in circulation (Dall'Acqua et al., 2002). The trend for the enhanced stabilities of H-FcRn:, C-FcRn: and M-FcRn:variant antibody complexes at pH 6.0 demonstrates that mutations in the C_H2 and C_H3 Fc regions affect FcRn binding. These results are consistent with previous reports indicating the involvement of these regions in interactions with FcRn (Burmeister et al., 1994a; Dall'Acqua et al., 2002; Kim et al., 1994; Kim et al., 1999; Martin et al., 2001; Medesan et al., 1996; Raghavan et al., 1994; Raghavan et al., 1995; Shields et al., 2001; Vaughn et al., 1997; Vaughn and Bjorkman, 1998; West and Bjorkman, 2000).

Overall, the variants we generated displayed affinity enhancements to the human, murine and monkey receptors of ~15- to 197-fold (Tables 1-3). These increases are

larger than observed in earlier studies which reported FcRn binding affinity enhancements with variant humanized IgGs from ~2- to 30-fold (Dall'Acqua et al., 2002; Hinton et al., 2004; Hinton et al., 2006; Shields et al., 2001). The increases in binding affinities were more marked for the interaction of the Fc variants with M-FcRn than H-FcRn, analogous with previous reports of the interaction of human IgGs with murine and human receptors (Dall'Acqua et al., 2002). The interaction of the WT anti-TNFα and the variants with C-FcRn was similar to H-FcRn (Figures 1A and 1B). Each of the Fc variant antibodies have comparable affinities for C-FcRn (K_D values of ~ 3 to 4 nM) and H-FcRn (K_D values of ~2 to 3 nM) at pH 6.0 (Tables 1 and 2), indicating these mutations in the gG backbone make similar free energy contributions to H-FcRn and C-FcRn binding. The association rate (k_{on} values) of the Fc variant antibody:C-FcRn complexes is ~20 to 30-fold faster than that of the WT antibody (Table 2). The dissociation rates (k_{off} values) of the three mutant antibody:C-FcRn complexes are similar to that (within ~2 to 3-fold) of the WT antibody:C-FcRn complexes at pH 6.0 (Table 2). The results indicate that the change in affinities of the variants are influenced more by the rate of association with C-FcRn.

The P257I/Q311I, P257I/N434H and D376V/N434H Fc variants have affinities (K_D values) for the murine receptor of ~5 nM, 1 nM and 7 nM, respectively (Table 3). Mutation of position 434 to a titratable residue (histidine) in the cases of D376V/N434H, and P257I/N434H increases the affinity of each IgG for M-FcRn ~17- and 197-fold, respectively, relative to the WT antibody. In crystal structure, the center of the FcRn:IgG binding interface includes a core of hydrophobic residues surrounded by a network of salt bridges. The Fc residues Q311 and N434 are at the border of the interface (Burmeister et

al., 1994a; Burmeister et al.,1994b; Vaughn and Bjorkman, 1998; West and Bjorkman, 2000). Mutations at these positions may increase the number of noncovalent interactions within the binding interface, which increases the affinity for FcRn. The Fc residues P257 and D376[2] are located in the C_H2-C_H3 interdomain region, but are not in direct contact with FcRn (Deisenhofer, 1981). Substitutions at these positions may indirectly affect interactions at the M-FcRn:Fc binding interface through differential influence on the interdomain angle. This is evident in the interactions of the variants D376V/N434H and P257I/N434H with M-FcRn. Although both variants contain the N434H[1] mutation, the P257I/N434H variant shows a more marked affinity enhancement for the murine receptor (~12-fold more) than D376V/N434H. Enhanced IgG:M-FcRn binding affinity was caused by either an increased association rate, slowed dissociation rate or a combination of both (Table 3). Each of the Fc variants showed a ~3- to 6-fold increase relative to the WT antibody in their rate of association with M-FcRn and also displayed ~3- to 30-fold slower rates of dissociation from the M-FcRn:antibody complexes compared to the WT molecule.

pH-dependent dissociation of H-FcRn:, C-FcRn: and M-FcRn:anti-TNFα antibody complexes

FcRn mediated IgG salvage begins with the interaction of IgG with FcRn which is facilitated by the acidic pH of the endosomal compartment (Ober et al., 2004b). However, the association and dissociation kinetics of the complex at various points in the intracellular recycling pathway and when the complex is exposed to the neutral pH of blood, may also affect the pharmacokinetic properties of monoclonal antibodies. To measure these parameters *in vitro,* we formed FcRn complexes with our anti-TNFα

antibodies at pH 6.0 and determined the extent of dissociation of the preformed complexes as the pH was increased using two independent methods; fluorescence anisotropy and ELISA. Fluorescence anisotropy is a solution based method, in which preformed IgG:FcRn complexes were titrated with base and exposed to each pH change in tandem. The ELISA is a solid phase method in which FcRn was immobilized to a plate surface. In contrast to the fluorescence anisotropy method, preformed IgG:FcRn complexes were exposed to a single pH change in the ELISA format.

The data from the pH-dependent dissociation of IgG:FcRn complexes was consistent between both assay formats (Figures 2 and 3). After formation of the H-FcRn:IgG and C-FcRn:IgG complexes at pH 6.0, the dissociation of the WT and variant molecules from the complex as the pH increased was very similar and characteristic of the Fc:FcRn interaction (Figures 2A and 2B). The H-FcRn: and C-FcRn:anti-TNFα antibody complexes dissociated with pH_{50} values of ~6.3 to 6.6 (Tables 1 and 2). At pH 7.4, ≥ 87% of the WT and each Fc variant antibody were dissociated from H-FcRn and C-FcRn (Figures 2A and 2B and Tables 1 and 2). In contrast, the pH at which preformed M-FcRn:IgG complexes dissociated varied significantly, with each of the variants showing decreased dissociation from preformed receptor complexes at neutral pH relative to the WT (Figures 2C and 3B). The pH_{50} at which P257I/Q311I:, D376V/N434H: and P257I/N434H:M-FcRn complexes dissociate are pH 7.3, 7.2 and 7.6, respectively, whereas the WT:M-FcRn complex has a pH_{50} value of 6.6. The majority of the WT IgG (> 90%) dissociates from M-FcRn at pH 7.4, while ~40 to 80% of the mutant antibodies remained bound to M-FcRn (Figure 2C and Table 3).

Pharmacokinetics of anti-TNFα WT and mutant antibodies in cynomolgus monkeys

In order to understand how the *in vitro* affinity differences observed for the variant IgG:C-FcRn interactions correlated to antibody kinetics *in vivo*, we investigated the pharmacokinetics of the WT and two of the variants (D376V/N434H and P257I/N434H) in cynomolgus monkeys after IV administration. The third variant (P257I/Q311I) was not studied *in vivo* as its binding characteristics were similar to the D376V/N434H and P257I/N434H variants. The WT and variants were cleared from the serum in a bi-phasic manner with similar serum profiles (Figure 4). No statistically relevant differences were observed between the WT and variant antibodies in total exposure, clearance, volume of distribution or $t_{1/2\beta}$ (Table 4). The WT antibody had a mean elimination $t_{1/2\beta}$ of 6 days, while the P257I/N434H and D376V/N434H variants had a mean $t_{1/2\beta}$ of 4.3 and 4.8 days, respectively (Table 4). There were no differences observed in the serum concentrations determined by the antigen capture or human IgG_1 ELISAs for the WT anti-TNFα or the variants indicating the antibodies were intact.

Pharmacokinetics of anti-TNFα WT and mutant antibodies in CD-1 mice

Due to the differences observed in the *in vitro* binding with M-FcRn and C-FcRn, we also examined the kinetics of the WT and three variants in CD-1 mice after IV administration. The WT antibody was cleared slowly (clearance value of 0.6 mL/h/kg) having an elimination $t_{1/2\beta}$ estimated at approximately 11.6 days (Table 5). Conversely, the D376V/N434H, P257I/N434H and P257I/Q311I variants distributed from the circulation extremely rapidly (Figure 5). The clearance of P257I/N434H appeared to be more extensive than for P257I/Q311I and D376V/N434H (Figure 5 and Table 5). The $t_{1/2\beta}$ of D376V/N434H, P257I/N434H and P257I/Q311I were estimated as 27, 8.6 and 28 hours (Table 5), respectively. Statistical analyses of the plasma concentrations of the Fc

variants at 24 hours post-dose and beyond were showed significant differences ($P < 0.01$) from wild-type. Analyses of the kinetics of the antibodies in B6 mice also showed the same rank order in clearance, exposure and $t_{1/2\beta}$, indicating the behavior of the molecules are not unique to the CD-1 murine strain (data not shown).

Discussion

In this report, we characterize differences in the IgG:FcRn interaction using H-FcRn, C-FcRn and M-FcRn and relate the observations to pharmacokinetics in mice and monkeys, using a series of humanized antibody Fc variants on an anti-TNFα IgG_1 antibody backbone. The *in vitro* FcRn binding properties of these molecules within and between species provided a unique opportunity to systematically assess how multiple binding parameters, either independently or in combination, influenced their *in vivo* kinetics.

In endothelial cells, FcRn diverts IgG from intracellular degradative pathways to a recycling compartment resulting in increased IgG serum persistence *in vivo* (Ober et al., 2004b; Ward et al., 2003). Simplistically, increasing the affinity of an antibody for FcRn at pH 6.0 would shift the equilibrium towards recycling in endosomal compartments and thereby translate to improved *in vivo* kinetics. Reports in the literature have suggested that there is a correlation between the serum $t_{1/2\beta}$ and binding affinity of an IgG for FcRn (Ghetie et al., 1997; Hinton et al., 2004; Hinton et al., 2006; Kim et al., 1994; Medesan et al., 1998). Although these investigations demonstrated that the FcRn binding affinity of an IgG correlates with increased serum $t_{1/2\beta}$, they presented fairly limited assessments and did not develop systematic *in vitro* binding property relationships for prediction of *in vivo* pharmacokinetics. For instance, in a rhesus monkey study, there is a fundamental gap in the direct relationship between the magnitude of receptor binding affinity enhancement and increased IgG serum persistence (Hinton et al., 2004). This discrepancy has also been observed in mice (Dall'Acqua et al., 2002; Ghetie et al., 1997; Gurbaxani et al., 2005; Medesan et al., 1998). These discrepant observations are probably related to other

aspects of the IgG:FcRn interaction, which were not characterized or controlled. In order to address these issues, multiple FcRn binding characteristics need to be measured. In addition to K_D, the interaction kinetics, relative binding at neutral and acidic pH and the affect of increasing pH on complex dissociation are factors which may need to be considered and balanced to translate *in vitro* observations to *in vivo* performance. The influences of the various *in vitro* binding parameters on *in vivo* kinetics may be different for IgG_1 molecules other than anti-TNFα, as well as, other IgG subtypes and other specific Fc variants.

Since the only difference in the *in vitro* C-FcRn binding properties of our IgGs was affinity at pH 6.0 (Table 2), we were able to evaluate the effect of this parameter on *in vivo* performance independent of other influences. In cynomolgus monkeys, we observed that the clearance and $t_{1/2\beta}$ of all the variant antibodies were similar to that of the WT antibody after IV administration (Figure 4). In rhesus monkeys, recent reports demonstrate humanized variant IgG_1 and IgG_2 molecules with ~30-fold increases in FcRn binding *in vitro* have two-fold increased serum persistence (Hinton et al., 2004; Hinton et al., 2006). Although we observed enhancements in binding affinity that were greater than or comparable to those of Hinton *et al*. (Hinton et al., 2004; Hinton et al., 2006) (Table 3), our mutations do not translate to an increased serum persistence. Because none of our variants bound to C-FcRn at pH 7.4 and all were released in a pH dependent fashion (Figure 2B), it is very unlikely that cell surface binding at neutral pH could have offset the benefit provided by the improved pH 6.0 binding. Others have suggested that the kinetics of dissociation at endosomal pH (pH 6.0) may influence antibody pharmacokinetics (Ghetie et al., 1997). The increased affinity of our variants for C-FcRn

was driven predominantly by an increase in association rate, with each displaying rates of dissociation from complexes similar to that of the WT molecule (Table 2). Since we did not observe improved *in vivo* properties of our variants in primates (Table 4 and Figure 4), one could speculate that, at the cellular level, the rate of dissociation of the FcRn:IgG complexes at endosomal pH may be an additional factor determining whether a preponderance of antibody is processed through the recycling or degradative pathways. While Hinton *et al*. did not report on the kinetics of binding of their molecules with FcRn (Hinton et al., 2004; Hinton et al., 2006), it is plausible that the affinity increase imparted by their mutation is driven by off rate kinetics which in turn leads to the observed pharmacokinetic benefit. Due to the similarity in binding interactions with C-FcRn and H-FcRn, it would be anticipated that our mutations on the anti-TNFα molecule would also not translate to pharmacokinetic benefit in humans (Tables 1 and 2). Overall, the results suggest that simply measuring the *in vitro* binding affinity at pH 6.0 is not the sole predictor of *in vivo* pharmacokinetics of these anti-TNFα variants.

The differential interactions of the anti-TNFα antibodies with M-FcRn allowed us to systematically examine the combined effect of these parameters using mice as the *in vivo* model. The P257I/N434H: and P257I/Q311I:M-FcRn complexes displayed rates of dissociation slower than the WT complex at pH 6.0 (Table 3); whereas the D376V/N434H complex has a k_{off} value similar to that of the WT IgG (Table 3). Based on our speculation around the influence of this parameter on intracellular trafficking and pharmacokinetics in primates, we expected that the slower rates of dissociation at pH 6.0 may drive a greater proportion of the IgG in these complexes (P257I/N434H and P257I/Q311I) to the recycling pathway compared with those having faster dissociation

kinetics (D376V/N434H and WT). This mechanism would result in the P257I/N434H and P257I/Q311I variants having a slower clearance and/or longer serum half-life in mice. However, after IV administration, the P257I/N434H, P257I/Q311I and D376V/N434H variants were cleared ~9 to 30 times faster than the WT antibody in mice, with the levels not measurable in plasma 24 to 96 hours after dosing. Others have also observed a rapid clearance of humanized Fc variants from circulation in mice which displayed enhanced affinity for M-FcRn at pH 6.0 *in vitro* (Dall'Acqua et al., 2002). In these studies, variants which had increased affinity for M-FcRn at pH 6.0 also displayed an uncharacteristic concomitant increase in affinity for the murine receptor at pH 7.4 (Dall'Acqua et al., 2002). It was speculated that the benefit of improved affinity at pH 6.0 was likely offset by the direct pH 7.4 binding, which allows IgGs to rebind to the receptor at the cell surface resulting in inefficient release into the circulation. Our humanized antibody variants are not acting through a rebinding mechanism at pH 7.4, since they showed no direct binding to M-FcRn at pH 7.4. In contrast to the C-FcRn observations, ~40 to 80% of our variant IgGs do not dissociate from preformed M-FcRn:variant complexes even after 30 minutes of incubation at neutral pH (Figure 2C). It is likely that the inability to dissociate from FcRn at neutral pH traps our variant anti-TNFα IgGs in the cell as the receptor complex recycles with the IgG still bound. This mechanism yields the poor pharmacokinetic profile of these molecules in mice, in a process that is distinct from the rebinding phenomenon at pH 7.4 (Dall'Acqua et al., 2002).

In summary, there are a number of parameters of the IgG:FcRn interaction that alone or in combination impact the *in vivo* clearance of our IgGs. Our studies clearly

demonstrate that changes in the pH dependency of complex dissociation appear to negatively impact the clearance of these variant anti-TNFα antibodies *in vivo*. Under either of these conditions it appears that the residence time of FcRn on cell surfaces is not long enough to allow significant proportions of the variants to dissociate from the complexes into the circulation. Because of their residence within FcRn containing tissues, such as the vasculature lining, these complexes may be capable of immune surveillance (Yoshida et al., 2004). Mechanistically, our variants may act as FcRn blockers that facilitate the degradation of endogenous IgGs *in vivo* (Vaccaro et al., 2005). Alternatively, the consequence of enhanced retention of the variants within the tissues could also lead to antibody degradation. Even without an influence on the pH dependency of the interaction as we observed in the primate, it is plausible that the acidic microenvironment created by Na^{+}-H^{+} exchange close to the endothelial cell surface (Claypool et al., 2004) results in slower release of high binding affinity IgGs from FcRn, offsetting the advantage of higher affinity binding observed at pH 6.0 (Lencer and Blumberg 2005; Ober et al., 2004a). The rank order in the increased clearance of the variants in mice parallels their dissociation behaviors from M-FcRn at pH 6.0 and 7.4, suggesting both of these phenomena influence the pharmacokinetics of the variants in mice. These studies have demonstrated that modification of FcRn:antibody interactions for optimization of pharmacokinetic properties *in vivo* more than likely involves the consideration of multiple factors in tandem including binding affinities, rates of interaction and pH-dependent dissociation. Understanding the relative influence of each of these factors on IgG kinetics, as well as, *in vitro* approaches which integrate these parameters would be valuable to directing therapeutic antibody engineering.

Acknowledgments

The authors thank Don McClure and Joseph Brunson for the expression of FcRn and anti-TNFα antibodies, Peng Luan for help with purification of the anti-TNFα antibodies, Fabian Tibaldi, Kevin Guo and Justin Recknor for performing the statistical analyses of the data and Nancy Goebl, Mary-Ann Campbell, Elaine Conner and Brian Ondek for helpful discussions.

References

Burmeister WP, Gastinel LN, Simister NE, Blum ML and Bjorkman PJ (1994a) Crystal structure at 2.2 A resolution of the MHC-related neonatal Fc receptor. *Nature* **372**:336-343.

Burmeister WP, Huber AH and Bjorkman PJ (1994b) Crystal structure of the complex of rat neonatal Fc receptor with Fc. *Nature* **372**:379-383.

Claypool SM, Dickinson BL, Wagner JS, Johansen FE, Venu N, Borawski JA, Lencer WI and Blumberg RS (2004) Bidirectional transepithelial IgG transport by a strongly polarized basolateral membrane Fcgamma-receptor. *Mol Biol Cell* **15**:1746-1759.

Dall'Acqua WF, Woods RM, Ward ES, Palaszynski SR, Patel NK, Brewah YA, Wu H, Kiener PA and Langermann S (2002) Increasing the affinity of a human IgG1 for the neonatal Fc receptor: biological consequences. *J Immunol* **169**:5171-5180.

Deisenhofer J (1981) Crystallographic refinement and atomic models of a human Fc fragment and its complex with fragment B of protein A from Staphylococcus aureus at 2.9- and 2.8-A resolution. *Biochemistry* **20**:2361-2370.

Ghetie V, Hubbard JG, Kim JK, Tsen MF, Lee Y and Ward ES (1996) Abnormally short serum half-lives of IgG in beta 2-microglobulin-deficient mice. *Eur J Immunol* **26**:690-696.

Ghetie V, Popov S, Borvak J, Radu C, Matesoi D, Medesan C, Ober RJ and Ward ES (1997) Increasing the serum persistence of an IgG fragment by random mutagenesis. *Nat Biotechnol* **15**:637-640.

Ghetie V and Ward ES (2000) Multiple roles for the major histocompatibility complex class I- related receptor FcRn. *Annu Rev Immunol* **18**:739-766.

Gurbaxani B, Dela Cruz LL, Chintalacharuvu K and Morrison SL (2005) Analysis of a family of antibodies with different half-lives in mice fails to find a correlation between affinity for FcRn and serum half-life. *Mol Immunol*

Hinton PR, Johlfs MG, Xiong JM, Hanestad K, Ong KC, Bullock C, Keller S, Tang MT, Tso JY, Vasquez M and Tsurushita N (2004) Engineered human IgG antibodies with longer serum half-lives in primates. *J Biol Chem* **279**:6213-6216.

Hinton PR, Xiong JM, Johlfs MJ, Tang MT, Keller S and Tsurushita N (2006) An Engineered Human IgG1 Antibody with Longer Serum Half-Life. *J Immunol* **176**:346-356.

Junghans RP and Anderson CL (1996) The protection receptor for IgG catabolism is the beta2-microglobulin-containing neonatal intestinal transport receptor. *Proc Natl Acad Sci USA* **93**:5512-5516.

Kim JK, Firan M, Radu CG, Kim CH, Ghetie V and Ward ES (1999) Mapping the site on human IgG for binding of the MHC class I-related receptor, FcRn. *Eur J Immunol* **29**:2819-2825.

Kim JK, Tsen MF, Ghetie V and Ward ES (1994) Identifying amino acid residues that influence plasma clearance of murine IgG1 fragments by site-directed mutagenesis. *Eur J Immunol* **24**:542-548.

Kunkel TA, Roberts JD and Zakour RA (1987) Rapid and efficient site-specific mutagenesis without phenotypic selection. *Methods in Enzymology* **154**:367-382.

Lencer WI and Blumberg RS (2005) A passionate kiss, then run: exocytosis and recycling of IgG by FcRn. *Trends Cell Biol* **15**:5-9.

Martin WL and Bjorkman PJ (1999) Characterization of the 2:1 complex between the class I MHC-related Fc receptor and its Fc ligand in solution. *Biochemistry* **38**:12639-12647.

Martin WL, West AP, Jr., Gan L and Bjorkman PJ (2001) Crystal structure at 2.8 A of an FcRn/heterodimeric Fc complex: mechanism of pH-dependent binding. *Mol Cell* **7**:867-877.

Medesan C, Cianga P, Mummert M, Stanescu D, Ghetie V and Ward ES (1998) Comparative studies of rat IgG to further delineate the Fc:FcRn interaction site. *Eur J Immunol* **28**:2092-2100.

Medesan C, Radu C, Kim JK, Ghetie V and Ward ES (1996) Localization of the site of the IgG molecule that regulates maternofetal transmission in mice. *Eur J Immunol* **26**:2533-2536.

Ober RJ, Martinez C, Lai X, Zhou J and Ward ES (2004a) Exocytosis of IgG as mediated by the receptor, FcRn: an analysis at the single-molecule level. *Proc Natl Acad Sci USA* **101**:11076-11081.

Ober RJ, Martinez C, Vaccaro C, Zhou J and Ward ES (2004b) Visualizing the site and dynamics of IgG salvage by the MHC class I-related receptor, FcRn. *J Immunol* **172**:2021-2029.

Raghavan M and Bjorkman PJ (1996) Fc receptors and their interactions with immunoglobulins. *Annu Rev Cell Dev Biol* **12**:181-220.

Raghavan M, Bonagura VR, Morrison SL and Bjorkman PJ (1995) Analysis of the pH dependence of the neonatal Fc receptor/immunoglobulin G interaction using antibody and receptor variants. *Biochemistry* **34**:14649-14657.

Raghavan M, Chen MY, Gastinel LN and Bjorkman PJ (1994) Investigation of the interaction between the class I MHC-related Fc receptor and its immunoglobulin G ligand. *Immunity* **1** :303-315.

Rodewald R (1976) pH-dependent binding of immunoglobulins to intestinal cells of the neonatal rat. *J Cell Bio* **71**:666-669.

Shields RL, Namenuk AK, Hong K, Meng YG, Rae J, Briggs J, Xie D, Lai J, Stadlen A, Li B, Fox JA and Presta LG (2001) High resolution mapping of the binding site on human IgG1 for Fc gamma RI, Fc gamma RII, Fc gamma RIII, and FcRn and design of IgG1 variants with improved binding to the Fc gamma R. *J Biol Chem* **276**:6591-6604.

Vaccaro C, Zhou J, Ober RJ and Ward ES (2005) Engineering the Fc region of immunoglobulin G to modulate in vivo antibody levels. *Nat Biotechnol* **23**:1283-1288.

Vaughn DE and Bjorkman PJ (1998) Structural basis of pH-dependent antibody binding by the neonatal Fc receptor. *Structure* **6**:63-73.

Vaughn DE, Milburn CM, Penny DM, Martin WL, Johnson JL and Bjorkman PJ (1997) Identification of critical IgG binding epitopes on the neonatal Fc receptor. *J Mol Biol* **274**:597-607.

Ward ES, Zhou J, Ghetie V and Ober RJ (2003) Evidence to support the cellular mechanism involved in serum IgG homeostasis in humans. *Int Immunol* **15**:187-195.

West AP, Jr. and Bjorkman PJ (2000) Crystal structure and immunoglobulin G binding properties of the human major histocompatibility complex-related Fc receptor. *Biochemistry* **39**:9698-9708.

Yoshida M, Claypool SM, Wagner JS, Mizoguchi E, Mizoguchi A, Roopenian DC, Lencer WI and Blumberg RS (2004) Human neonatal Fc receptor mediates transport of IgG into luminal secretions for delivery of antigens to mucosal dendritic cells. *Immunity* **20**:769-783.

Footnotes

Send reprint requests to: Victor J. Wroblewski, Lilly Research Laboratories, Eli Lilly & Company, Lilly Corporate Center, Indianapolis, IN 46285, Phone: (317) 276-9306, Fax: (317) 276-4218, Email: wroblewski_victor@lilly.com

[1]Residues are numbered according to the Eu numbering system. P257I/Q311I indicates mutation of both Pro^{257} to Ile^{257} and Glu^{311} to Ile^{311}. P257I/N434H indicates mutation of both Pro^{257} to Ile^{257} and Asn^{434} to His^{434}. D376V/N434H indicates mutation of both Asp^{376} to Val^{376} and Asn^{434} to His^{434}.

[2]Residues are numbered according to the Eu numbering system. P257 indicates residue Pro^{257}. D376 indicates residue Asp^{376}.

Legends for Figures

Fig. 1. BIAcore sensorgrams of the interaction of WT anti-TNFα and the P257I/N434H variant with H-FcRn (A), C-FcRn (B) and M-FcRn (C) at pH 6.0. Sensorgrams display the response values for two measurements at the antibody concentrations of 0.0033 μM to 4.0 μM .

Fig. 2. pH-dependent dissociation of IgG:FcRn complexes by ELISA. The WT anti-TNFα (●) and the P257I/N434H (■), D376V/N434H (▲) and P257I/Q311I (□) variants were allowed to bind biotinylated H-FcRn (A), C-FcRn (B) and M-FcRn (C) captured on a streptavidin coated plate at pH 6.0 and dissociated at the pH values indicated. The amount of each antibody which remained bound was detected with HRP-conjugated goat F(ab')2 anti-human IgG. The curves are the mean ± SD of three measurements. The amount of antibody which remained bound at each pH is expressed as a percentage of the total antibody bound at pH 6.0.

Fig. 3. Fluorescence anisotropy binding and pH-dependent dissociation measurements of the WT (●) and P257I/N434H (■) anti-TNFα antibodies to Alexa 488-labeled C-FcRn (A) and M-FcRn (B). Antibody were allowed to bind Alexa 488-labeled FcRn at pH 6.0 and increasing amounts of 0.25 M NaOH were added, while monitoring the pH and change in anisotropy. The titration curves are the mean ± SD of two measurements. The amount of antibody which remained bound at each pH is expressed as a percentage of the total antibody bound at pH 6.0.

Fig. 4. Pharmacokinetic profiles of the WT anti-TNFα (○) and the P257I/N434H (■) and D376V/N434H (▲) variants in cynomolgus monkeys. Antibodies were administered as a single IV injection of 0.5 mg/kg. Data are the concentrations of the WT anti-TNFα and the P257I/N434H and D376V/N434H variants determined from serum samples at the indicated time points using a validated antigen capture (with TNFα) ELISA. Data are the mean ± SD of three animals/group.

Fig. 5. Pharmacokinetic profiles of the WT anti-TNFα (●) and the P257I/N434H (■), D376V/N434H (▲) and P257I/Q311I (□) variants in CD-1 mice. Antibodies were administered as a single IV injection of 1.0 mg/kg. Data are the concentrations of the WT anti-TNFα and the P257I/Q3111I, P257I/N434H and D376V/N434H variants determined from plasma samples at the indicated time points using a validated antigen capture (with TNFα) ELISA. Each time point represents the average plasma concentration for three or four mice over the course of the concentration versus time profile determined thru non-serial sampling. Plasma concentrations of the Fc variants at 24 hours post-dose and beyond were statistically significant ($P < 0.01$) from wild-type.

TABLE 1

Binding of humanized anti-TNFα antibodies to H-FcRn.

	Wild-type	P257I/N434H	D376V/N434H	P257I/Q311I
K_D[a] (nM)	37 ± 5	2.3 ± 0.2[*]	2.5 ± 1.4[*]	1.9 ± 0.4[*]
pH_{50}[b]	6.6 ± 0.2	6.6 ± 0.1	6.5 ± 0.1	6.6 ± 0.1
% Bound pH 7.4[c]	13 ± 2	6 ± 2	6 ± 1	9 ± 2

[a]K_D data determined from equilibrium analysis of two independent binding experiments and expressed as the mean ± SD.

[b]pH at which 50% of the IgG:H-FcRn complexes dissociates as determined from a four-parameter nonlinear regression fit (described in the Materials and Methods) of the ELISA data.

[c]Percentage of the total antibody in preformed complexes which remained FcRn bound at pH 7.4 as determined by ELISA.

[*]$P < 0.001$ compared to wild-type

DMD Fast Forward. Published on October 18, 2006 as DOI: 10.1124/dmd.106.011734
This article has not been copyedited and formatted. The final version may differ from this version.

TABLE 2

Binding of humanized anti-TNFα antibodies to C-FcRn.

	Wild-type	P257I/N434H	D376V/N434H	P257I/Q311I
K_D[a] (nM)	209 ± 11	4.0 ± 0.7*	4.0 ± 0.3*	2.6 ± 0.5*
k_{on} (x 10^6)(1/M•s)	0.22	4.3	5.0	6.5
k_{off} (x 10^{-2})(1/s)	4.6	1.7	2.0	1.7
$t_{1/2}$[b] (min)	0.25	0.68	0.58	0.68
pH_{50}[c]	6.3 ± 0.1	6.5 ± 0.1	6.3 ± 0.1	6.5 ± 0.2
% Bound pH 7.4[d]	0.5 ± 3	10 ± 4	3 ± 1	7 ± 2

[a]K_D data determined from kinetic analysis two independent binding experiments and expressed as the mean ± SD ($K_D = k_{off}/k_{on}$•1 x10^9)

[b]Half-life of the IgG:FcRn complexes at pH 6.0 ($t_{1/2} = (\ln 2/k_{off})/60$)

[c]pH at which 50% of the IgG:C-FcRn complexes dissociates as determined from a four-parameter nonlinear regression fit (described in the Materials and Methods) of the ELISA data.

[d]Percentage of the total antibody in preformed complexes which remained FcRn bound at pH 7.4 as determined by ELISA.

*$P < 0.001$ compared to wild-type

DMD Fast Forward. Published on October 18, 2006 as DOI: 10.1124/dmd.106.011734
This article has not been copyedited and formatted. The final version may differ from this version.

TABLE 3

Binding of humanized anti-TNFα antibodies to M-FcRn.

	Wild-type	P257I/N434H	D376V/N434H	P257I/Q311I
K_D[a] (nM)	118 ± 7	0.6 ± 0.1*	7.1 ± 0.4*	4.7 ± 0.9*
k_{on} (x 10^6)(1/M•s)	0.39	2.5	2.1	1.3
k_{off} (x 10^{-2})(1/s)	4.6	0.16	1.5	0.61
$t_{1/2}$[b] (min)	0.25	7.2	0.77	1.9
pH_{50}[c]	6.6 ± 0.1	7.6 ± 0.1*	7.2 ± 0.1*	7.3 ± 0.2*
% Bound pH 7.4 [d]	6 ± 3	79 ± 2	37 ± 2	49 ± 2

[a]K_D data determined from kinetic analysis two independent binding experiments and expressed as the mean ± SD ($K_D = k_{off}/k_{on}$•1 x10^9)

[b]Half-life of the IgG:FcRn complexes at pH 6.0 ($t_{1/2} = (\ln 2/k_{off})/60$)

[c]pH at which 50% of the IgG:M-FcRn complexes dissociates as determined from a four-parameter nonlinear regression fit (described in the Materials and Methods) of the ELISA data.

[d]Percentage of the total antibody in preformed complexes which remained FcRn bound at pH 7.4 as determined by ELISA.

*$P < 0.002$ compared to wild-type

TABLE 4

Pharmacokinetic parameters for the humanized WT anti-TNFα and the P257I/N434H and D376V/N434H variants in male cynomolgus monkeys after IV administration of 0.5 mg/kg[a,b].

	Wild-type	P257I/N434H	D376V/N434H
C_{max} (μg/mL)	20 ± 14	13 ± 3	23 ± 5
$AUC_{0-\infty}$ (μg•hr/mL)	484 ± 118	410 ± 67	368 ± 83
CL (mL/h/kg)	1.1 ± 0.3	1.2 ± 0.2	1.4 ± 0.3
V_{ss} (mL/kg)	115 ± 21	122 ± 29	175 ± 12*
$t_{1/2\beta}$ (h)	144 ± 18	102 ± 13*	116 ± 11

$AUC_{0-\infty}$, area under the plasma concentration curve from zero to infinity; C_{max}, maximal observed plasma concentration; CL, clearance; V_{ss}, volume of distribution at steady state; $t_{1/2\beta}$, elimination half-life.

[a]Serum concentrations determined using a validated antigen capture (with TNFα) ELISA.

[b]Data are the mean ± SD of the pharmacokinetic parameters determined from three monkeys per group.

*P< 0.05 compared to wild-type

TABLE 5

Pharmacokinetic parameters for the humanized WT anti-TNFα and the P257I/N434H, D376V/N434H and P257I/Q311I variants in male CD-1 mice after IV administration of 1.0 mg/kg[a,b].

	Wild-type	P257I/N434H	D376V/N434H	P257I/Q311I
C_{max} (μg/mL)	16.4	5.1	11.2	8.5
$AUC_{0-\infty}$ (μg•hr/mL)	1682	49	261	186
CL (mL/h/kg)	0.6	20	3.6	5.3
V_{ss} (mL/kg)	226	253	140	219
$t_{1/2\beta}$ (h)	279	8.6	27	28

$AUC_{0-\infty}$, area under the plasma concentration curve from zero to infinity; C_{max}, maximal observed plasma concentration; CL, clearance; V_{ss}, volume of distribution at steady state; $t_{1/2\beta}$, elimination half-life.

[a]Plasma concentrations determined using a validated antigen capture (with TNFα) ELISA.

[b]Pharmacokinetic parameters are determined from the mean plasma concentration data from three or four mice per group.

DMD Fast Forward. Published on October 18, 2006 as DOI: 10.1124/dmd.106.011734
This article has not been copyedited and formatted. The final version may differ from this version.

Figure 1

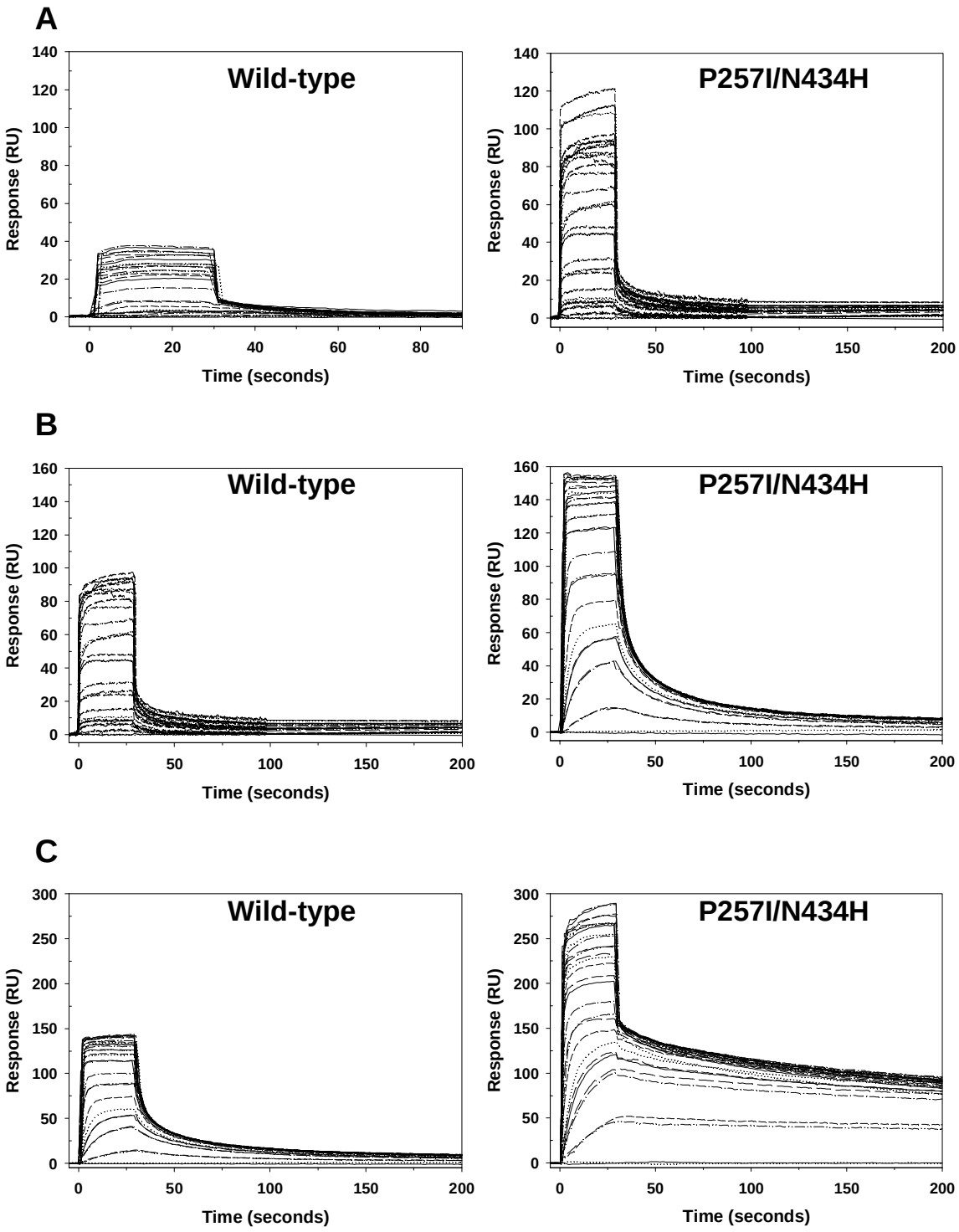

DMD Fast Forward. Published on October 18, 2006 as DOI: 10.1124/dmd.106.011734
This article has not been copyedited and formatted. The final version may differ from this version.

Figure 2

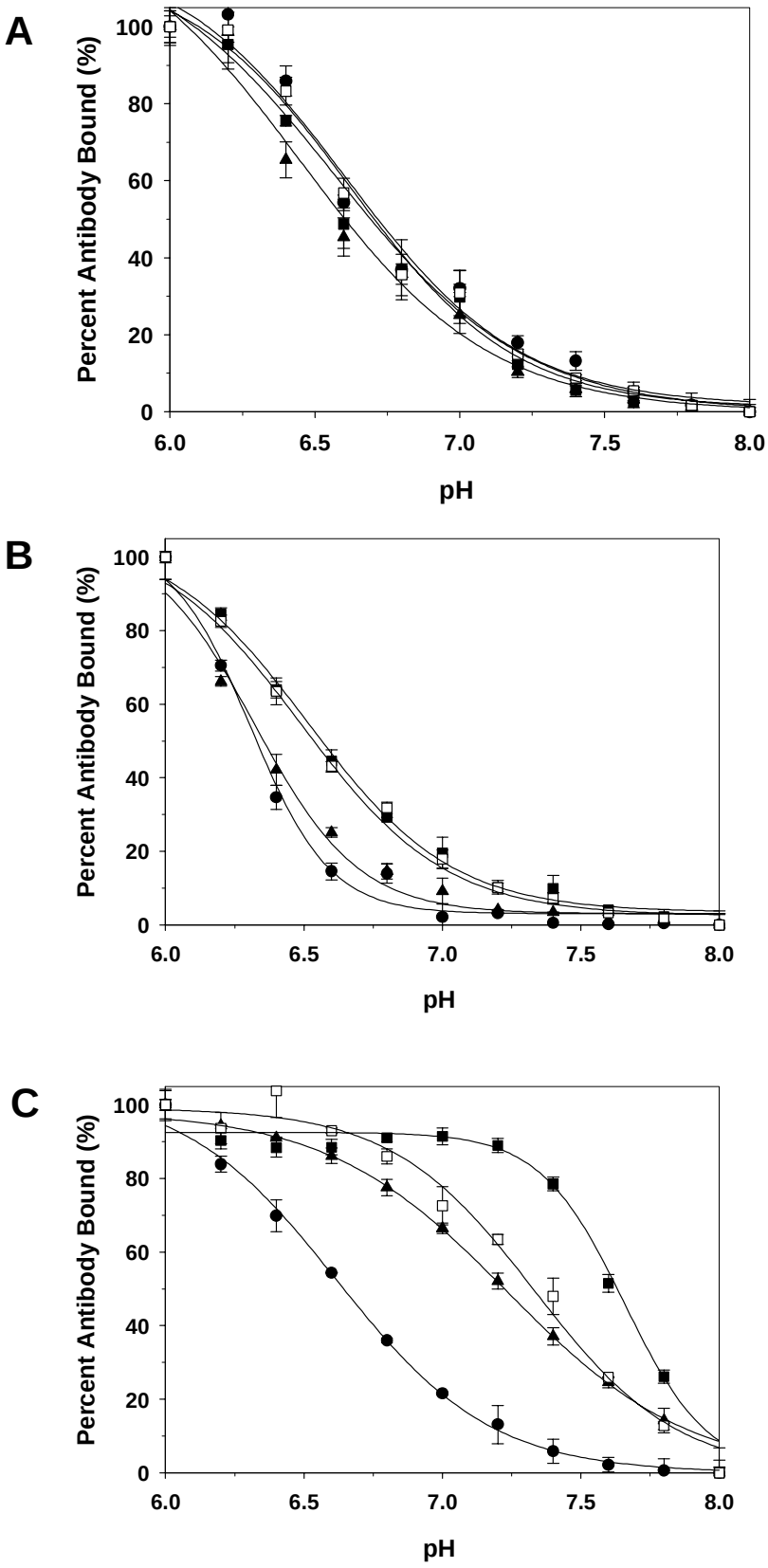

DMD Fast Forward. Published on October 18, 2006 as DOI: 10.1124/dmd.106.011734
This article has not been copyedited and formatted. The final version may differ from this version.

Figure 3

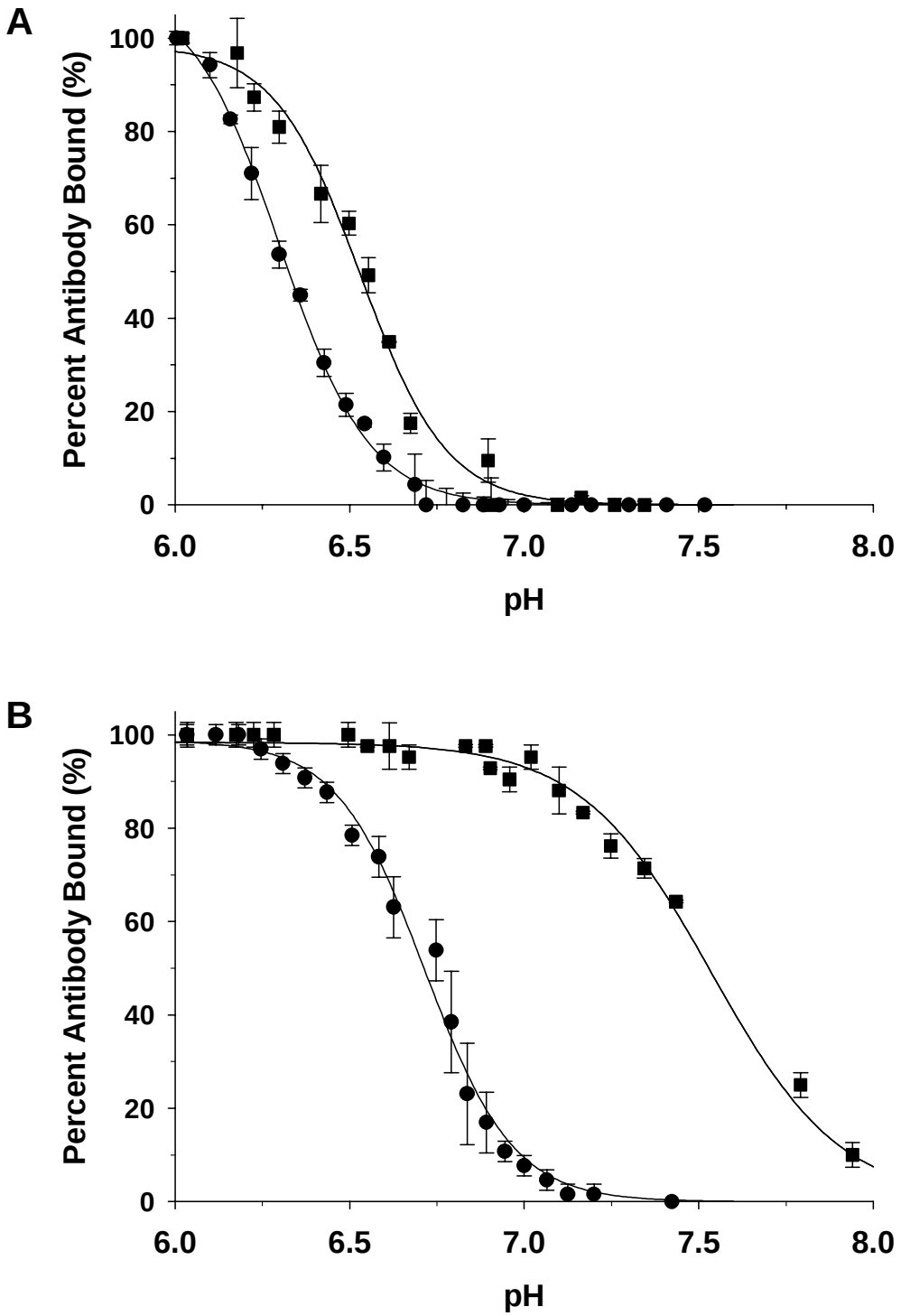

DMD Fast Forward. Published on October 18, 2006 as DOI: 10.1124/dmd.106.011734
This article has not been copyedited and formatted. The final version may differ from this version.

Figure 4

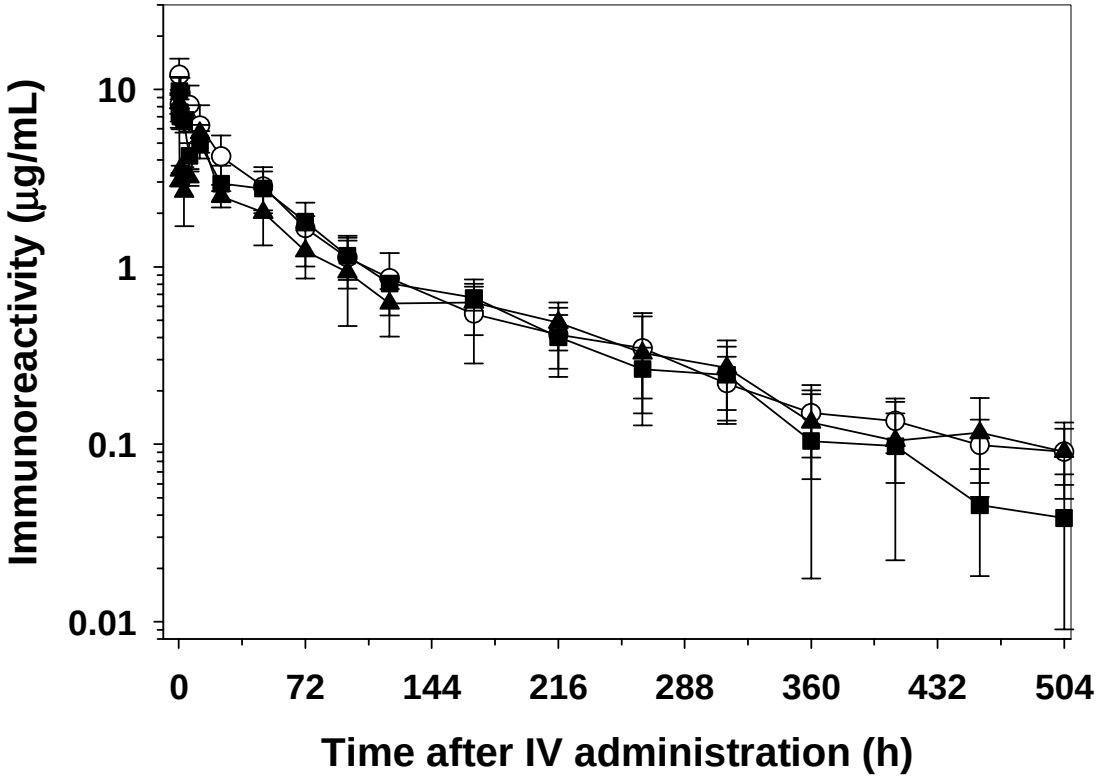

DMD Fast Forward. Published on October 18, 2006 as DOI: 10.1124/dmd.106.011734
This article has not been copyedited and formatted. The final version may differ from this version.

Figure 5